Sulfoxide-functionalized Graphitic Carbon Nitride-Cobalt Dialkyl Phosphate Bipyridine Heterojunction for Photocatalytic Hydrogen Production

Navneet Matharoo, Mohammed Fawaz, Nithinraj Panangattu Dharmarajan, Ayona K Jose, Jae-Hun Yang, Matej Huš, *CI Sathish, Xuan Minh Chau Ta, Harleen Kaur, Yuwei Wang, Antonio Tricoli, Prashant Kumar,* Blaž Likozar, *Ramaswamy Murugavel*, Ajayan Vinu**

Navneet Matharoo, Mohammed Fawaz, Nithinraj Panangattu Dharmarajan, Jae-Hun Yang, Harleen Kaur, Ayona K Jose, Yuwei Wang, Prashant Kumar, Ajayan Vinu*

Global Innovative Center for Advanced Nanomaterials, College of Engineering, Science and Environment (CESE), The University of Newcastle, University Drive, Callaghan 2308, NSW, Australia. Email:Ajayan.Vinu@newcastle.edu.au

Navneet Matharoo, Ramaswamy Murugavel *

Department of Chemistry, Indian Institute of Technology Bombay, Mumbai 400076, India.

Email: rmv@chem.iitb.ac.in

Xuan Minh Chau Ta, Antonio Tricoli,

Nanotechnology Research Laboratory, Faculty of Engineering, University of Sydney, Sydney 2006, NSW, Australia

Yuwei Wang

State Key Laboratory of Clean Energy Utilization, Zhejiang University, Hangzhou 310027, China.

Prashant Kumar

University of Petroleum and Energy Studies (UPES), Dehradun, Uttarakhand, 248007, India

Matej Huš, Blaž Likozar

Department of Catalysis and Chemical Reaction Engineering, National Institute of Chemistry, Ljubljana 1000, Slovenia

Keywords: Sulfoxide-functionalized, carbon nitride, metal-diorganophosphate, hybridization, photocatalysis, hydrogen evolution reaction.

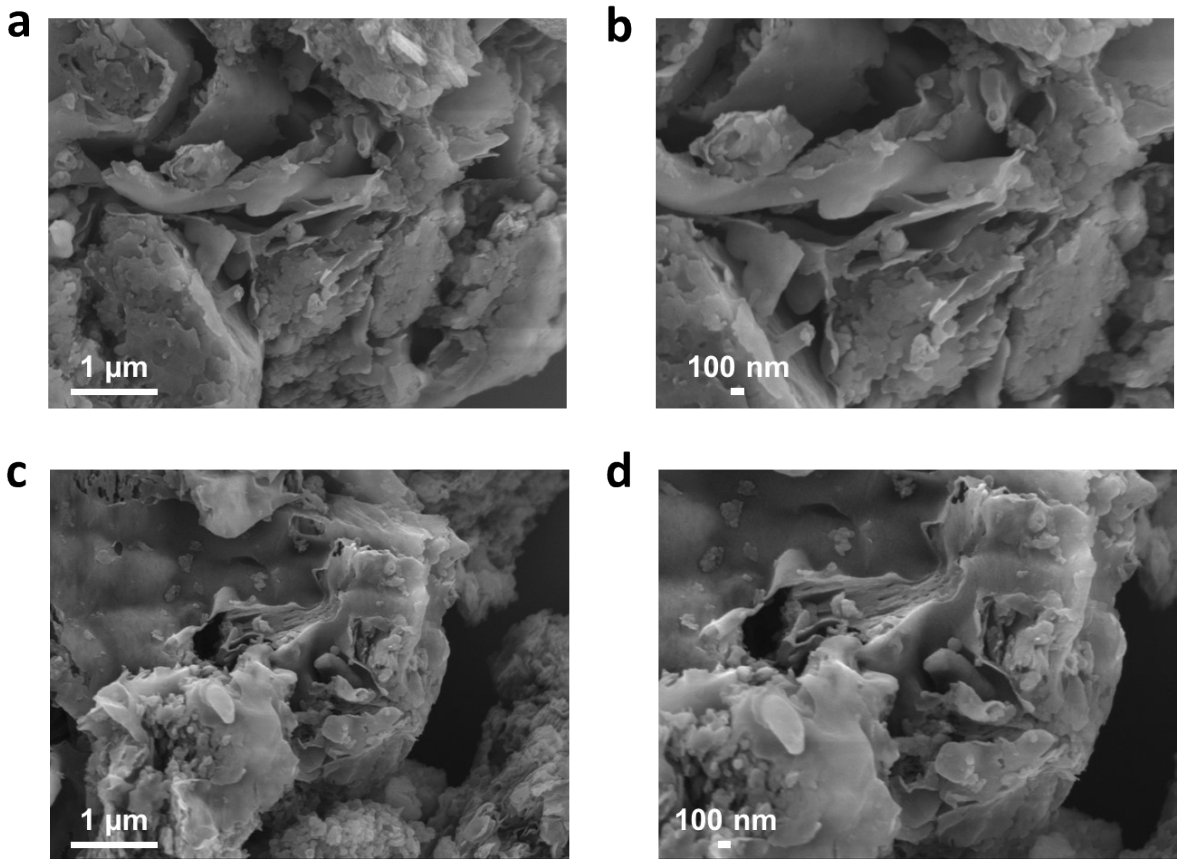

Fig. S1 SEM image of (a, b) SCN-CP-1 and (c, d) SCN-CP-3.

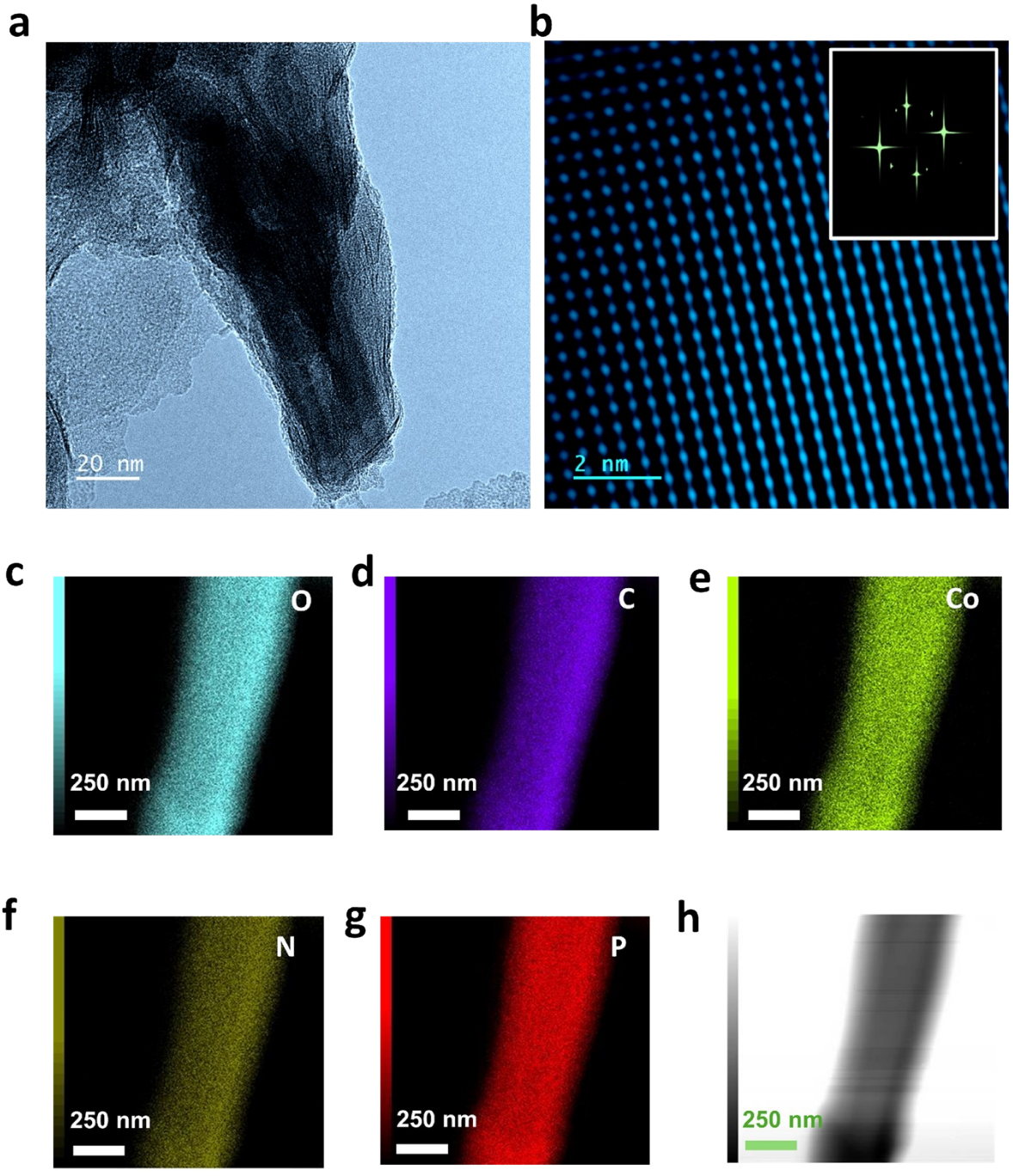

Fig. S2 (a) TEM, (b) HRTEM (inset FFT), (c-h) elemental profile for O, C, Co, N, P, and SEI of CP.

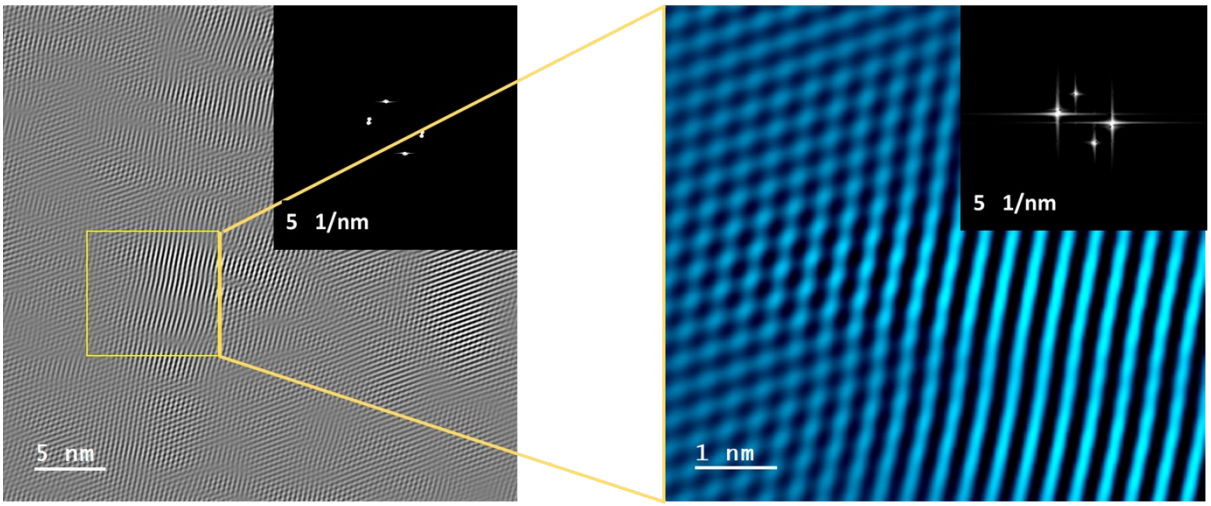

Fig. S3 TEM (left) and HRTEM (right) (d, e) atomistic line profiles along marked directions, (f) SEI pattern and (g-k) elemental profile for C, P, Co, N and O of SCN-CP-3.

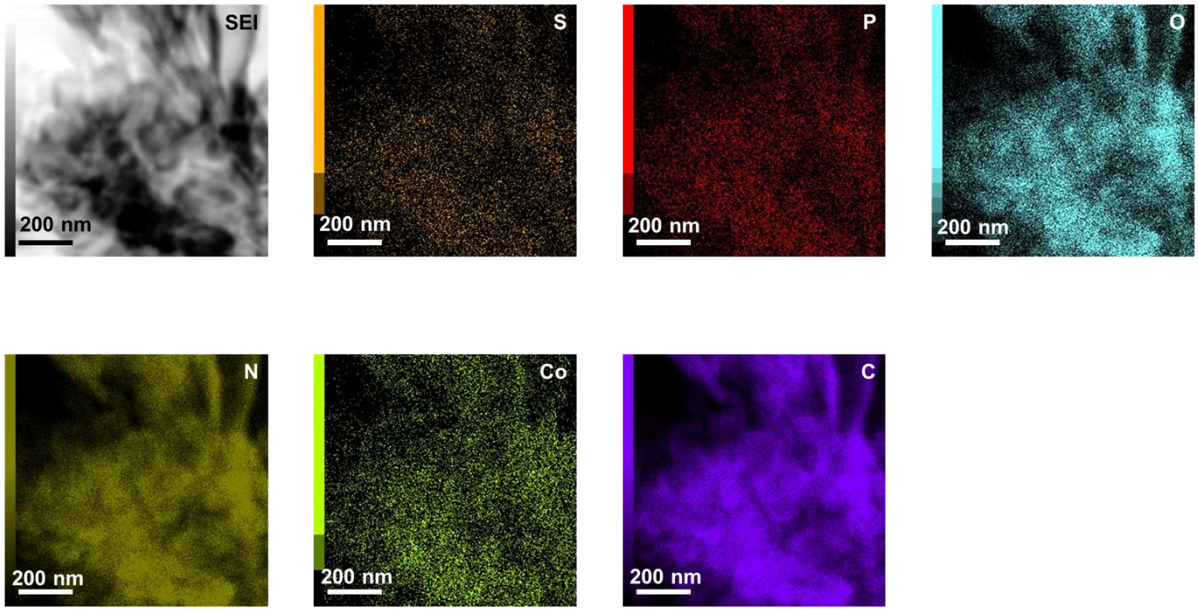

Fig. S4 (a) TEM, (b, c) HRTEM, (d, e) atomistic line profiles along marked directions, (f) SEI pattern and (g-k) elemental profile for C, P, Co, N and O of SCN-CP-3.

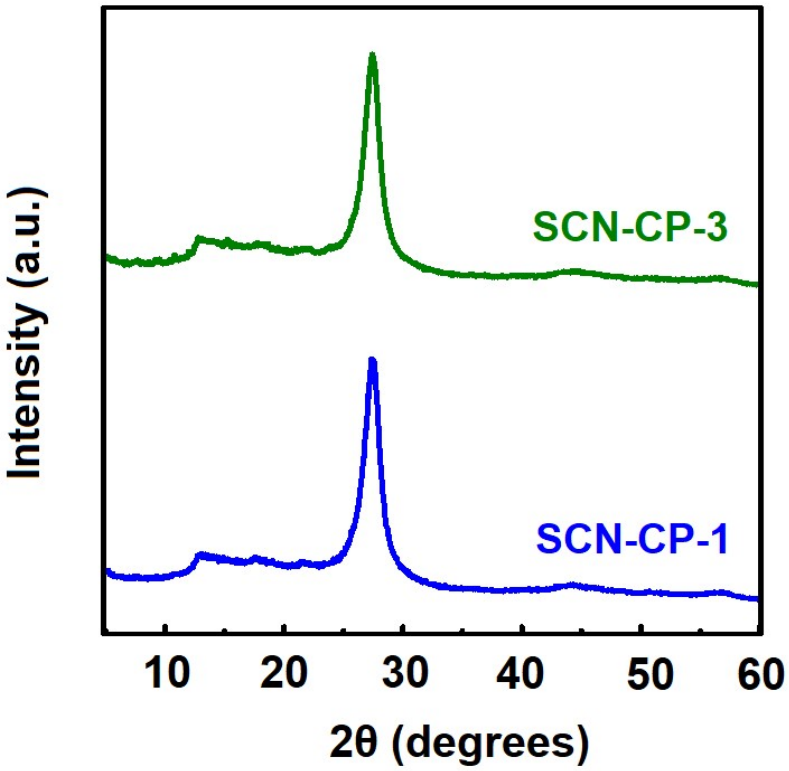

Fig. S5 PXRD patterns of SCN-CP-1 and SCN-CP-3 hybrids.

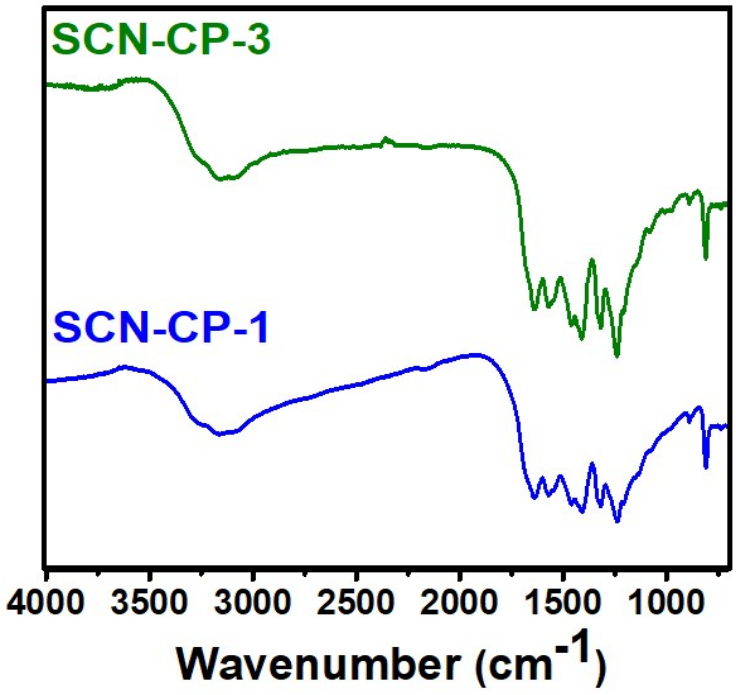

Fig. S6 FTIR spectra of SCN-CP-1 and SCN-CP-3 hybrids.

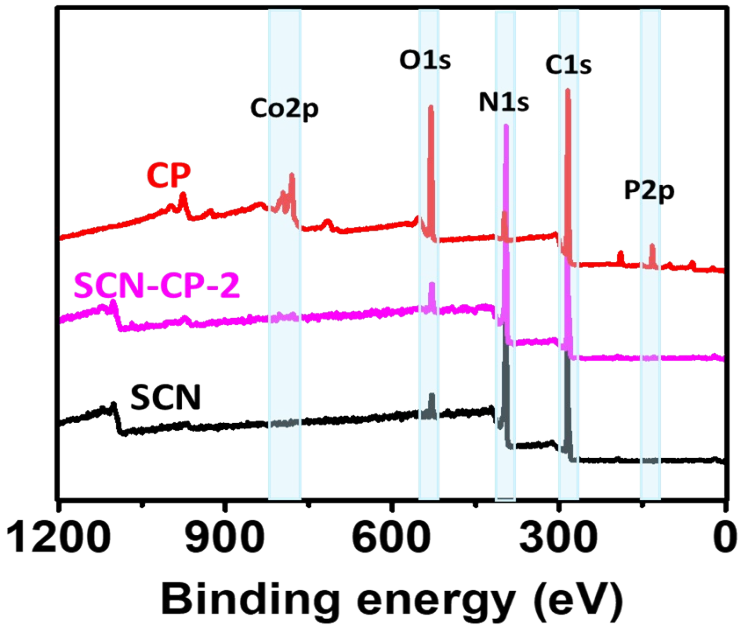

Fig. S7 XPS Survey spectrum of SCN, CP and SCN-CP-2.

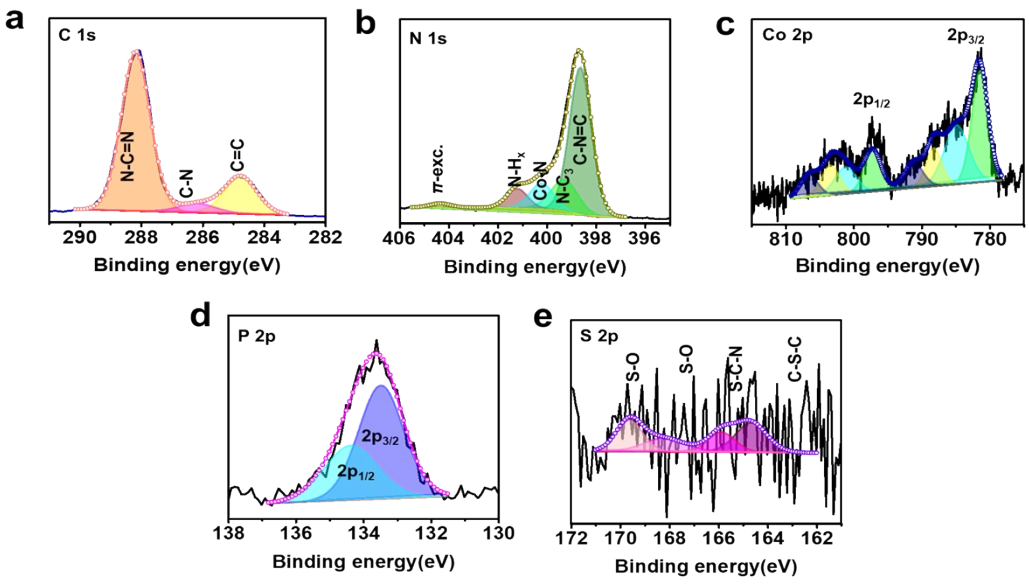

Fig. S8 High resolution spectrum of (a) C 1s, (b) N 1s, (c) Co 2p, (d) P2p and (e) S 2p of SCN-CP-3.

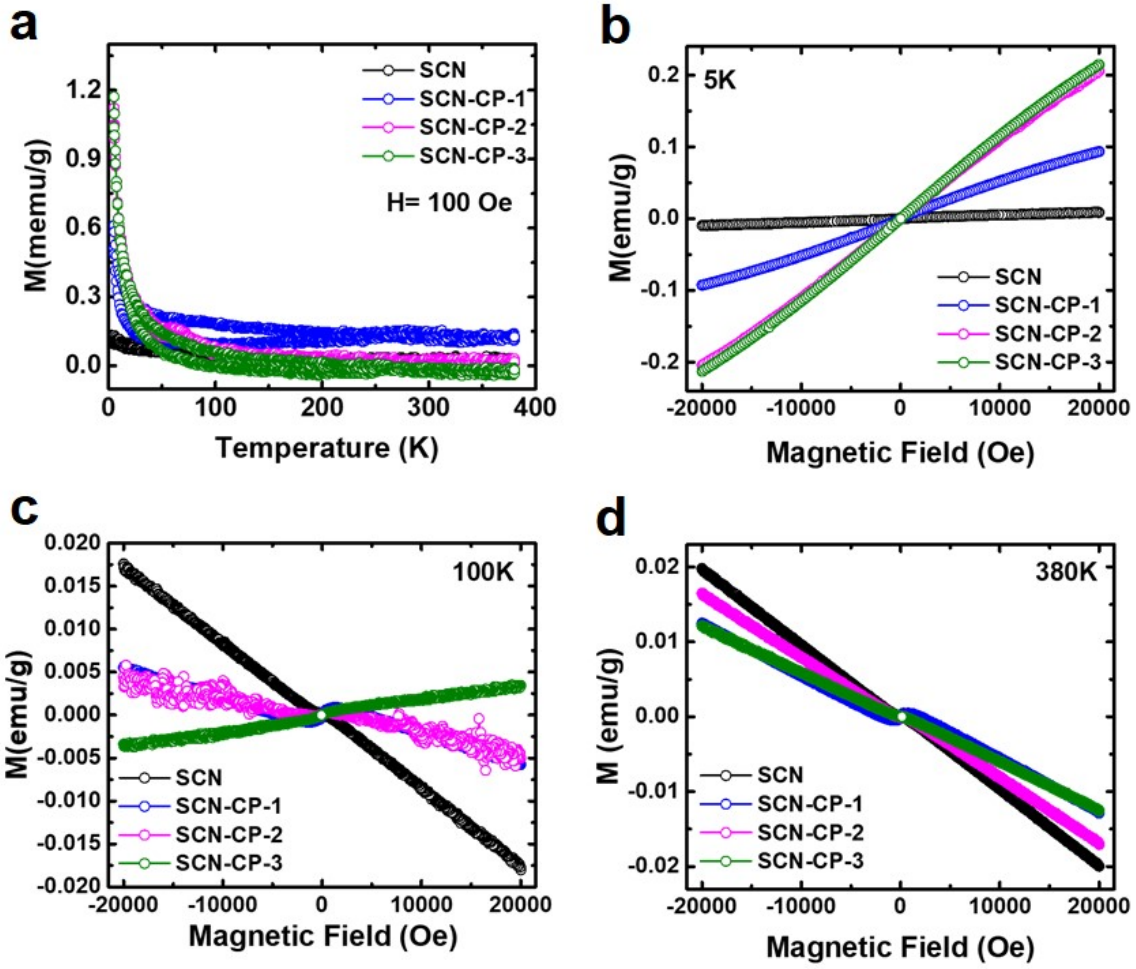

Fig. S9 (a) ZFC-FC curves of SCN-CP hybrids , magnetic hysteresis (*M-H*) loops at (b) 5 K, (c) 100 K and (d) 300 K.

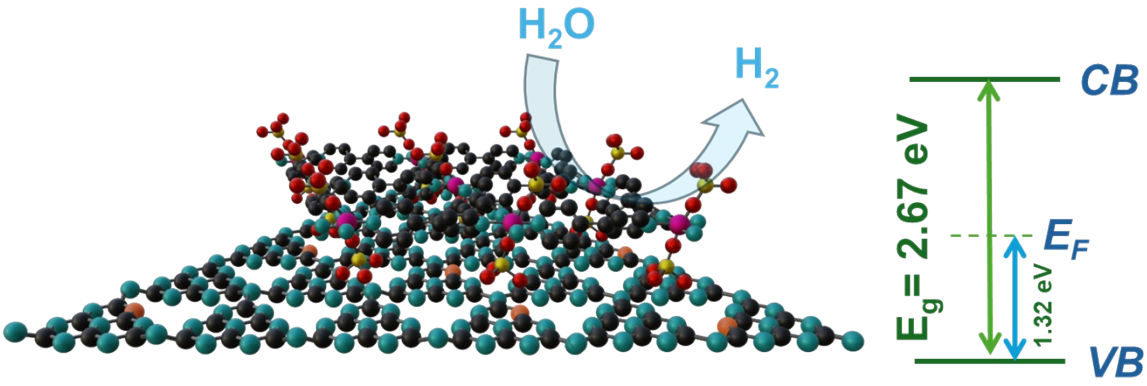

Fig. S10 Schematic diagram depicting photocatalytic HER performance of SCN-CP hybrids.

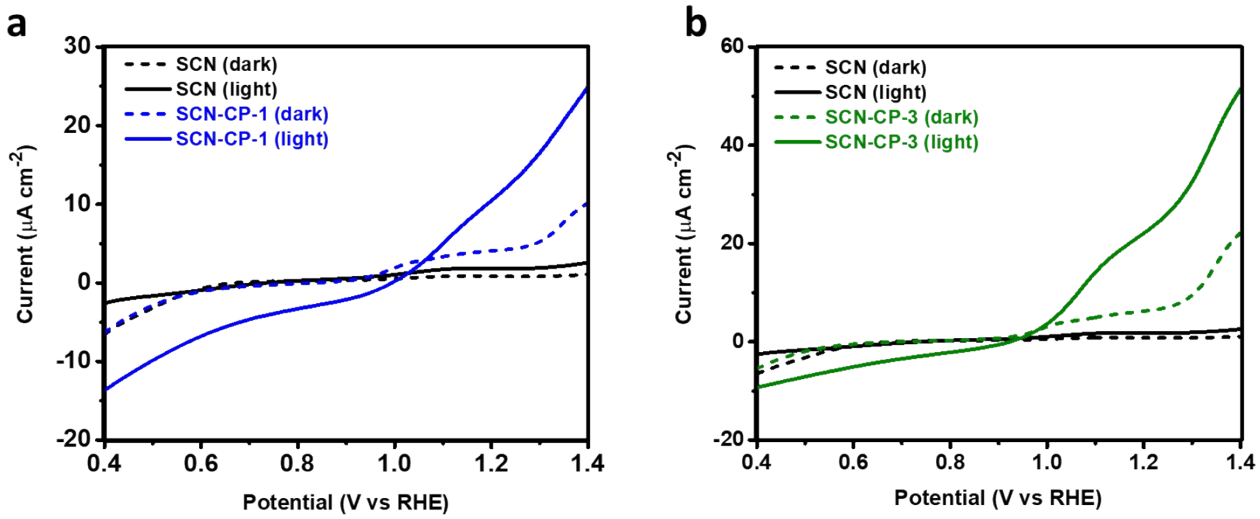

Fig. S11 Linear sweep voltammetry curves for (a) SCN-CP-1 and (b) SCN-CP-3.

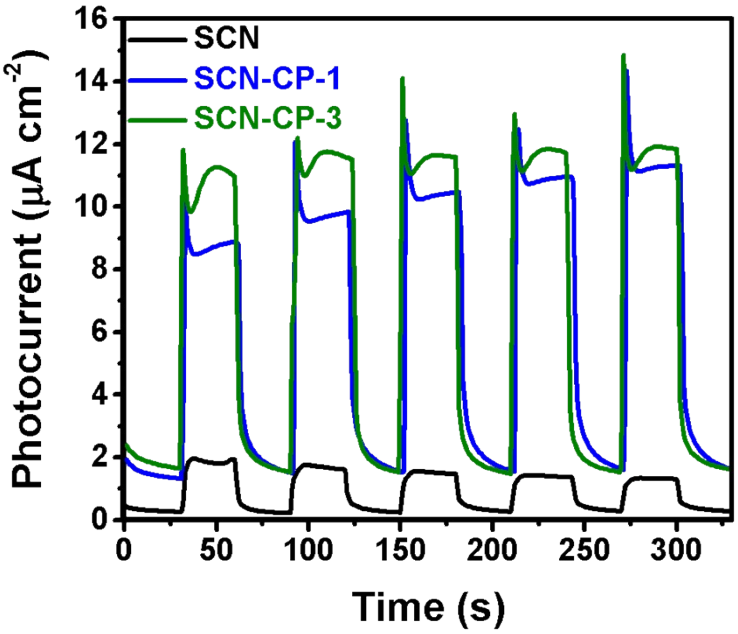

Fig. S12 Photocurrent response under the periodic on/off of visible light ($\lambda \geq 400$ nm) for SCN, SCN-CP-1 and SCN-CP-3.

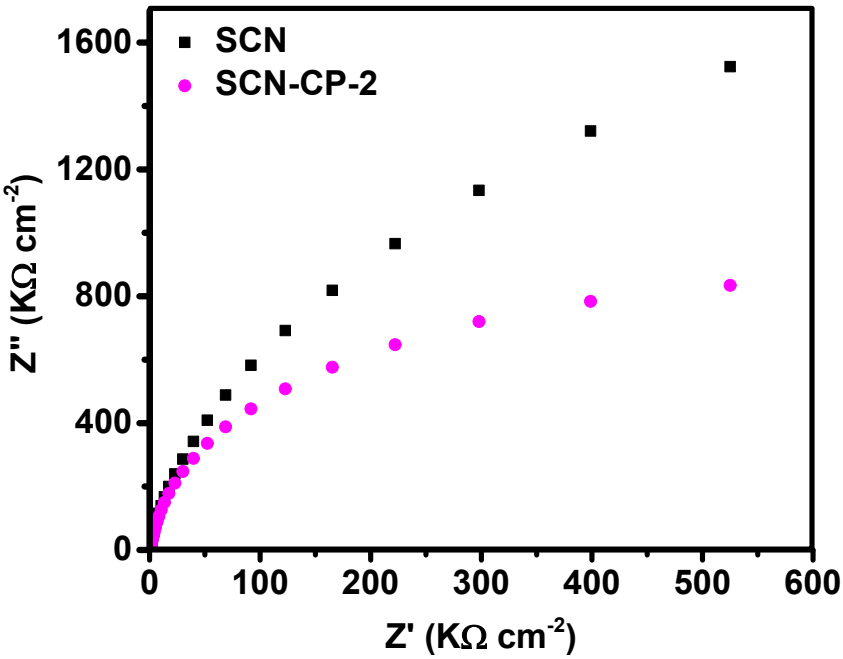

Fig. S13 EIS Nyquist plots of the SCN and SCN-CP-2.

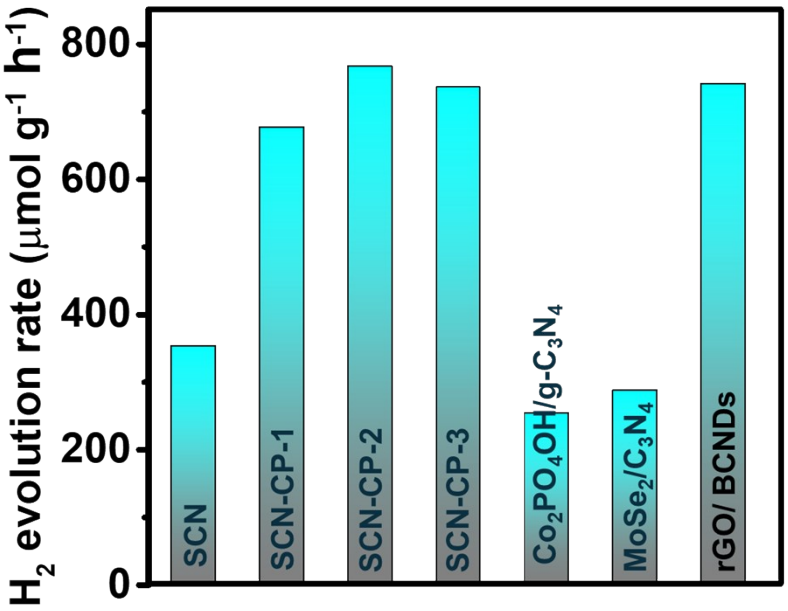

Fig. S14 Hydrogen evolution rate of SCN, CDTBP and SCN-CP hybrids along with reported heterostructures.

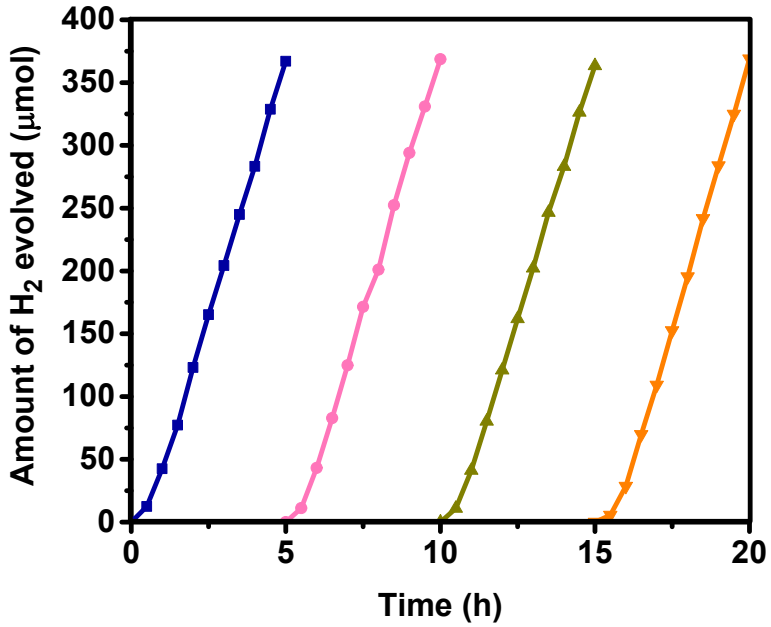

Fig. S15 The long-term stability test of **SCN-CP-2** for 20 hours with evacuation every 5 hours.

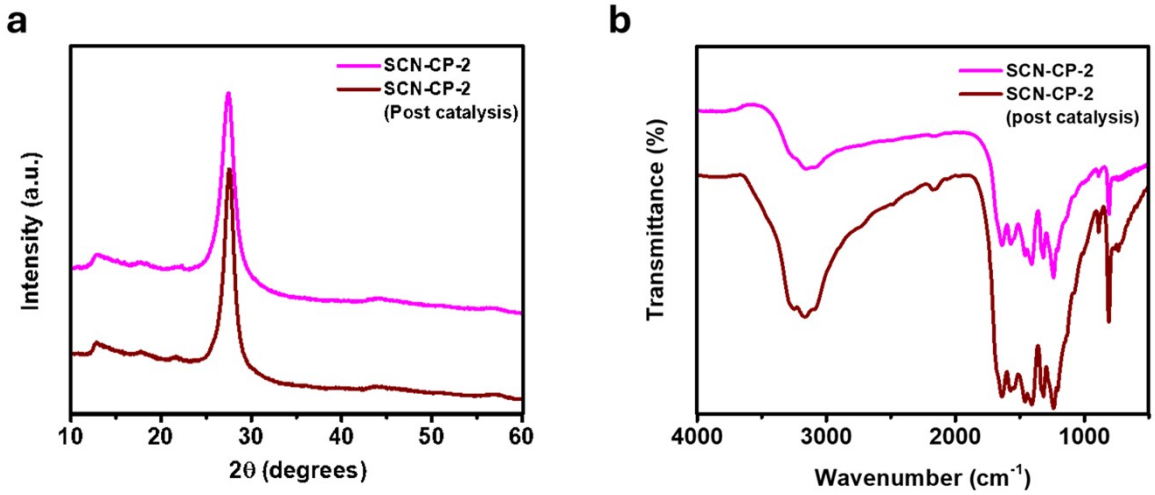

Fig. S16 Post catalysis (a) PXRD and (b) FT-IR of SCN-CP-2 after four HER cycles.

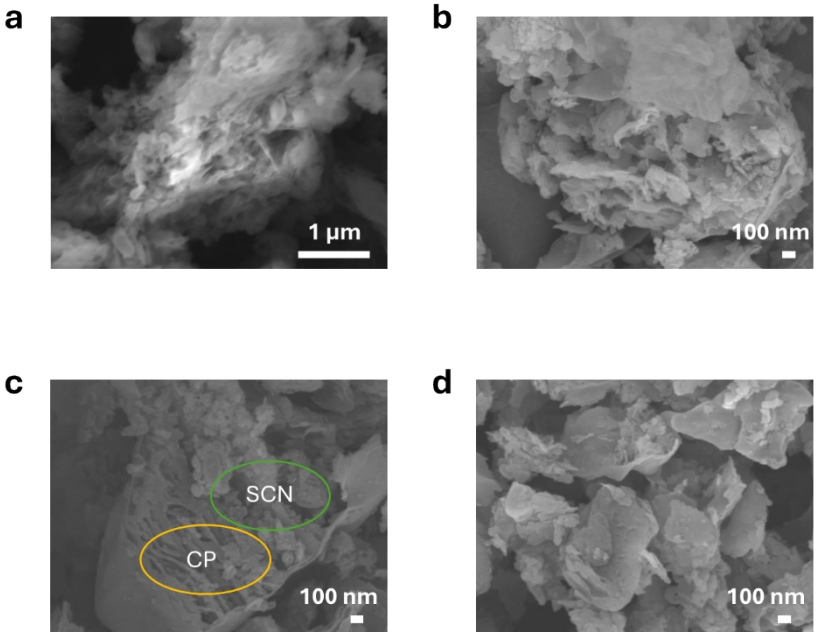

Fig. S17 (a-d) Post catalysis SEM images of SCN-CP-2 showing the coexistence of SCN and CP grid, confirming the preservation of morphology after prolonged photocatalysis.

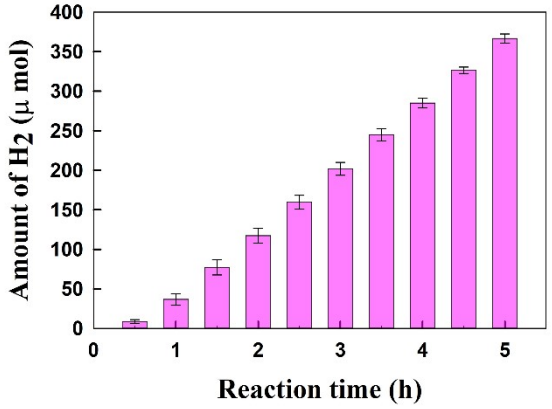

Fig. S18 H_2-evolution profile of **SCN-CP-2** under visible-light irradiation. Each point represents the average of four independent measurements, and the error bars indicate the corresponding variations.

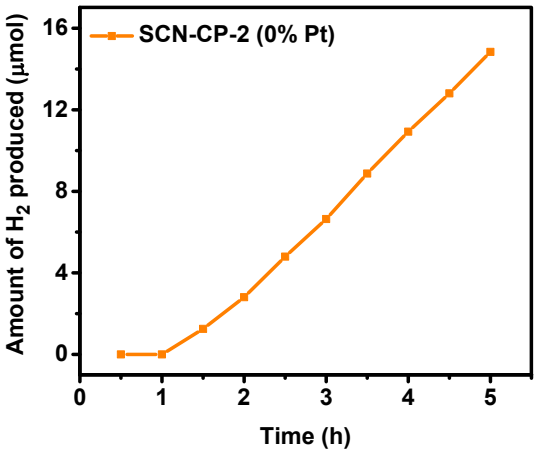

Fig. S19 Control experiment for photocatalytic HER without Pt cocatalyst.

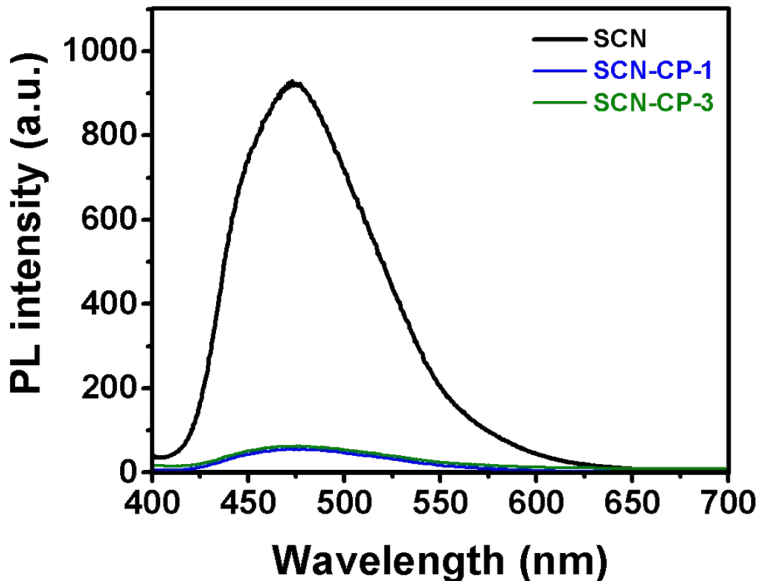

Fig. S20 PL spectra (λ_{ex} = 375 nm) of SCN, SCN-CP-1 and SCN-CP-3.

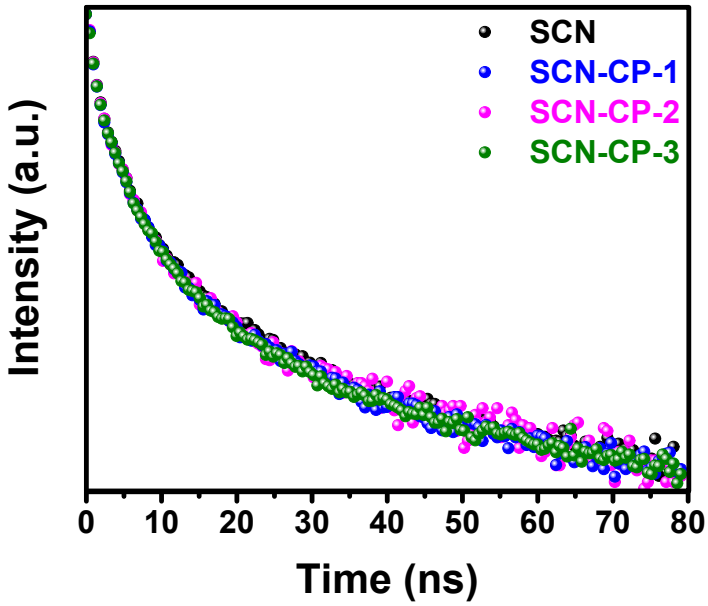

Fig. S21 TRPL spectra of **SCN**, **SCN-CP-1**, **SCN-CP-2** and **SCN-CP-3**.

Table S1. The evolution rate of H_2 of SCN and its hybrid with various concentrations of CP in the photocatalytic hydrogen evolution reaction.

Sample	H_2 evolution rate (μmol g^{-1} h^{-1})	Amount of H_2 evolved in 5h (μmol g^{-1})
SCN	353.2	1668.2
SCN-CP-1	677.1	3215.9
SCN-CP-2	828.0	3740.0
SCN-CP-3	736.3	3463.5

Table S2. Comparison of photocatalytic hydrogen evolution rates of representative g-C_3N_4 based and cobalt/sulfur-modified photocatalysts.

S.No.	Catalyst	H_2 evolution rate	Reference
1.	S-CN	55.2 μmol$g^{-1}h^{-1}$	1
2.	CNQDs/CoPi-2	254 μmol$g^{-1}h^{-1}$	2
3.	GCP-5	254 μmol$g^{-1}h^{-1}$	3
4.	g-C_3N_4/CoO	651.3 μmol$g^{-1}h^{-1}$	4
5.	CoS_2- S-g-C_3N_4	550 μmol$g^{-1}h^{-1}$	5
6.	CDs/CoO/g-C_3N_4	987.4 μmol$g^{-1}h^{-1}$	6
7.	CoO/CoP/g-C_3N_4	1277.9 μmol$g^{-1}h^{-1}$	7
8.	TiO_2	364.2 μmol$g^{-1}h^{-1}$	8
9.	P25(degussa)	96.5 μmol$g^{-1}h^{-1}$	8
10.	$Co(OH)_2$/g-C_3N_4/$Ni(OH)_2$	899 μmol$g^{-1}h^{-1}$	9
11.	**SCN**	353.2 μmol$g^{-1}h^{-1}$	This work
12.	**SCN-CP-2**	828.0 μmol$g^{-1}h^{-1}$	This work

References:

1 T. M. Khedr, S. M. El-Sheikh, M. Endo-Kimura, K. Wang, B. Ohtani and E. Kowalska, *Nanomaterials*, 2023, **13**, 62.

2 Z. Liu, Xing Hu, Longxin Zhang, Yujie Lai, Hua Peng, Gang Li, Junhua Zeng, Rongying Yi, *Photochem. Photobiol.*, 2024, **100**, 22–32.

3 S. K. Lakhera, V. S. Vijayarajan, B. S. Rishi Krishna, P. Veluswamy and B. Neppolian, *Int. J. Hydrogen Energy*, 2020, **45**, 7562–7573.

4 Z. Mao, J. Chen, Y. Yang, D. Wang, L. Bie and B. D. Fahlman, *ACS Appl. Mater. Interfaces*, 2017, **9**, 12427–12435.

5 Y. Zhang, J. Shi, Z. Huang, X. Guan, S. Zong, C. Cheng, B. Zheng and L. Guo, *Chem. Eng. J.*, 2020, **401**, 126135.

6 W. Shi, J. Wang, S. Yang, X. Lin, F. Guo and J. Shi, *J. Chem. Technol. Biotechnol*, 2020, **95**, 2129–2138.

7 Y. Han, Zh. Wang, X. Yang, Z. Li and Y. Li, *Catalysts*, 2025, **15**, 315.

8 D. Wang, P. Kanhere, M. Li, Q. Tay, Y. Tang, Y. Huang, T. C. Sum, N. Mathews, T. Sritharan and Z. Chen, *J. Phys. Chem. C*, 2013, **117**, 22894–22902.

9 J. Zhang, S. Shao, D. Zhou, T. Di and T. Wang, *ACS Appl. Energy Mater.*, 2021, **4**, 6340–6347.